JCTC
Journal of Chemical Theory and Computation

Article

Validation of Pseudopotential Calculations for the Electronic Band Gap of Solids

Pedro Borlido, Jan Doumont, Fabien Tran, Miguel A. L. Marques,* and Silvana Botti*

Read Online

ACCESS | Metrics & More | Article Recommendations | Supporting Information

ABSTRACT: Nowadays pseudopotential (PP) density functional theory calculations constitute the standard approach to tackle solid-state electronic problems. These rely on distributed PP tables that were built from all-electron atomic calculations using few popular semilocal exchange-correlation functionals, while PPs based on more modern functionals, such as meta-generalized gradient approximation and hybrid functionals, or for many-body methods, such as GW, are often not available. Because of this, employing PPs created with inconsistent exchange-correlation functionals has become a common practice. Our aim is to quantify systematically the error in the determination of the electronic band gap when cross-functional PP calculations are performed. To this end, we compare band gaps obtained with norm-conserving PPs or the projector-augmented wave method with all-electron calculations for a large data set of 473 solids. We focus, in particular, on density functionals that were designed specifically for band gap calculations. On average, the absolute error is about 0.1 eV, yielding absolute relative errors in the 5−10% range. Considering that typical errors stemming from the choice of the functional are usually larger, we conclude that the effect of choosing an inconsistent PP is rather harmless for most applications. However, we find specific cases where absolute errors can be larger than 1 eV or others where relative errors can amount to a large fraction of the band gap.
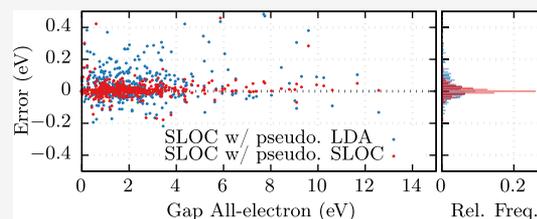
INTRODUCTION

Since its origin more than 50 years ago, density functional theory[1,2] (DFT) has become the standard approach to tackle the electronic structure of solids. A workable approach to DFT is attained via the Kohn−Sham formulation,[2] leading to equations that can be solved efficiently with modern computational resources. Although DFT is in principle exact, it relies on approximations of the exchange-correlation (xc) energy functional, which inherently limits the accuracy of calculations.[3−8]

From a purely theoretical point of view, the xc functional is the only approximation in DFT. However, in practice, the Kohn−Sham equations—a system of coupled, nonlinear, and partial differential equations—are solved numerically, introducing further approximations. Several different approaches have been developed and are commonly used in the physics and chemistry communities. A basic distinction exists between all-electron and pseudopotential (PP) (or effective-core potential) methods. In the former, all electrons are explicitly included in the calculation, and the electron−nuclear attraction is described by the standard Coulomb potential. The latter method is based on the distinction between core and valence electrons. By replacing the effect of the nucleus and the core electrons by an effective PP, efficient plane-wave[9] or real-space[10,11] techniques can be used to solve the Kohn−Sham equations. As a middle way, the projector-augmented wave (PAW) method[12,13] was developed, combining the advantages of PPs with a reconstruction of the all-electron wave function. Another alternative, the hybrid Gaussian and plane-wave density-functional scheme,[14,15] can also be considered intermediate

between PP and all-electron methods. One should keep in mind, however, that PP and PAW implementations usually rely on the frozen-core approximation, that is, the inner core orbitals remain fixed to their atomic values and are not allowed to polarize under the effect of the valence electrons or the other atoms. Furthermore, PPs and PAW setups are normally calculated from atomic density-functional calculations performed with a specific xc functional and should therefore be only used in calculations performed with the same functional.

In materials science, DFT calculations are often performed with these effective-core methods.[16,17] Well-tuned PPs can reproduce very precisely all-electron results for many properties of solids[18−20] but at a much lower computational cost. However, in order to guarantee this, careful optimization is necessary to ensure the quality and transferability of the PP for the situation at hand. Several well-tested tables are available to the community, but all these PPs are built based on two approximations to the xc energy functional, the local density approximation (LDA)[21−24] and the generalized gradient approximation (GGA), and, more specifically, the Perdew−Burke−Ernzerhof (PBE)[25] functional, which is the *de facto*

standard in the physics community. This is true for norm-conserving[26] and ultrasoft[27] PPs and for the PAW method.[12] The disparity between the number of functionals in generally available PP data sets (LDA, PBE, and sometimes PBEsol[28]) and the number of available xc functionals in the literature[29,30] (more than 500) is therefore confounding, especially if we consider that *ab initio* PPs have been well established since the late 70's[26,31−35] and that recently developed xc functionals have been acknowledged to be more accurate for electronic structure calculations than standard LDA and GGA functionals.[36−40] As a result of this situation, the great majority of calculations performed with improved functionals make use of an inconsistent PP, built from LDA or PBE atomic calculations. This problem is relevant for both total-energy and band-structure calculations. For the latter, which are the focus of the present work, the most accurate calculations use either hybrid functionals (such as the Heyd−Scuseria−Ernzerhof 2006 functional[39,40]), GW methods,[41,42] or specialized semilocal functionals, such as the modified Becke−Johnson potential[43] (mBJLDA). For example, despite the publication of several studies on the generation of PPs for Hartree−Fock and hybrid functionals,[44−49] the lack of readily available tables means that most of these calculations are performed with PBE ones. Furthermore, some codes do not give the user the possibility of changing the PPs. The situation is even more complicated for the mBJLDA potential as it is defined for periodic systems and cannot be applied to atoms, unless specific schemes are used.[50,51] Note that a similar problem exists also for many-body GW[41,42] or LDA + U[52,53] calculations that are often performed with LDA or PBE PPs.

This common practice creates an inconsistency, which invariably introduces some uncontrollable errors in the calculations. Even if this is well known, relatively little attention has been given up to now to quantify the effect of cross-functional PP calculations.[47,50,54−56] With this in mind, we decided to study the error coming from using an inconsistent PP in the calculation of band gaps. This was carried out by comparing the results obtained with three codes: WIEN2k,[57,58] an all-electron code that uses the augmented plane wave plus local orbital (APW + lo) method,[59] ABINIT[60,61] with norm-conserving PPs, and VASP[13,62] with PAW setups. Note that our comparison goes beyond the Δ test,[17] as we compare band gaps, which also include the influence of unoccupied bands, and we take into account errors coming from using inconsistent PPs.

■ METHODS

Data Set. We performed calculations for all materials contained in the data set developed in ref 63 which counts 473 nonmagnetic semiconductors. This data set covers the majority of the periodic table and includes materials with a wide range of band gaps. All calculations were performed at the experimental geometry (see ref 63 for more details on the material data set).

Functionals. Besides the standard LDA and PBE functionals, our choice of xc functionals (or potentials) was based on two criteria: (i) their availability in the three software packages that we used (see below for more information on the codes) and (ii) their relevance for the calculation of band gaps.

Our final choice includes the Perdew−Wang (PW92)[23] and the Perdew−Zunger (PZ81)[22] parametrization of the LDA correlation and the local Slater potential (SLOC).[64] We also consider several GGA functionals: PBE,[25] revised PBE (RPBE),[65] Engel−Vosko (EV93)[66] combined with the

Perdew−Wang (PW91) correlation,[67] and high local exchange (HLE16).[68] Finally, we consider the meta-GGA mBJLDA.[43]

Among the selected functionals, SLOC and HLE16 are less known and deserve a short description. The "simple local model for the Slater exchange potential" (SLOC)[64] has the same form as the LDA exchange

$$v_x(\mathbf{r}) = -an^b(\mathbf{r}) \tag{1}$$

where $n = \sum_j^{occ} |\psi_j|^2$ is the electron density. This functional uses two parameters $a = 1.67$ and $b = 0.3$, fitted to the Slater potential[69] of a series of closed-shell atoms. The high local exchange functional[68] (HLE16) is obtained by modifying the weights of the exchange and correlation terms of HCTH/407,[70] with the objective to improve the Kohn−Sham band gaps. Specifically, the exchange term is multiplied by 1.25 and the correlation term is multiplied by 0.5.

The PW92, PZ81, and PBE functionals are general-purpose approximations with widespread use in the solid-state community for total-energy calculations. The mBJLDA potential is known to yield excellent band gaps, which is also the case of the simpler SLOC and HLE16, although they are slightly inferior to mBJLDA.[63,71] Note that meta-GGA energy functionals are not supported self-consistently in the reference APW + lo WIEN2k code, and therefore, we did not include the recent meta-GGAs HLE17[72] and TASK,[73] which also perform very well for band gaps, in our analysis. Hybrid functionals are available in the three considered codes; however, they lead to calculations that are several orders of magnitude more expensive, in particular, if parameters for highly converged calculations are used. Therefore, because our test set is very large, we refrained from using hybrid functionals in the present work. For the same reason, we did not consider GW methods.

Codes. The all-electron calculations were performed with the WIEN2k package,[57,58] which uses the APW + lo basis set.[59] The calculations were performed with sufficiently stringent parameters to ensure well-converged results. In the vast majority of cases, the convergence error is less than 0.03 eV, but it can be larger for systems with very large band gaps. The number of **k**-points was defined by testing progressively denser meshes, and the parameter $R_{MT}^{min}K_{max}$ (the product of the smallest of the atomic sphere radii R_{MT} and the plane wave cutoff parameter K_{max}), which determines the size of the basis set, was chosen to be between 8 and 9 for most systems. For systems with very small atomic spheres, $R_{MT}^{min}K_{max}$ was reduced to a smaller value. The accurate WIEN2k results serve as a reference for the comparison with the other codes. As WIEN2k calculations were converged to 0.03 eV, values that differ by less than this quantity should be considered equivalent.

The PAW calculations were performed using a custom version of the Vienna ab initio simulation package (VASP; version 5.4)[13,62] that is interfaced to LIBXC.[29,30] A plane-wave cutoff of 520 eV was used for all species along with the same **k**-grids, as in ref 63. All meta-GGA calculations were performed accounting for nonspherical contributions of the density gradient inside the augmentation spheres. VASP calculations are, in general, restricted to the PAW sets included in the distribution, and therefore, we were able to use only PBE and LDA PAW PPs. The choice of how many electrons to include in the valence was carried out following the recommendations of the Materials Project database.[74]

The ABINIT package[60,61] was used to test norm-conserving PP calculations. For LDA and PBE PPs, we resorted to the Pseudo Dojo distribution[75] (version 0.4, with stringent

Table 1. M(A)E (in eV), Standard Deviation (in eV), M(A)PE (in %, for Band Gaps Larger Than 0.25 eV), and Maximum Absolute Error (in eV) with Respect to the All-Electron Results Obtained with the Considered Functionals When a Standard (LDA or PBE) PP is Used

|		ME	MAE	σ	MPE	MAPE	max. err.
ABINIT	LDA@LDA	0.01	0.02	0.04	0.45	2.47	−0.28 (SnTe)
	SLOC@LDA	0.05	0.08	0.14	3.13	5.43	1.33 (LaF$_3$)
	PBE@PBE	0.01	0.02	0.06	0.82	2.31	0.19 (GeAs)
	RPBE@PBE	0.01	0.03	0.04	0.98	2.89	−0.30 (SnTe)
	EV93@PBE	0.03	0.06	0.08	2.26	4.51	0.36 (ZnO)
	HLE16@PBE	0.06	0.10	0.14	3.57	6.50	1.10 (LaF$_3$)
VASP	LDA@LDA	0.01	0.03	0.04	0.93	2.96	−0.27 (SnTe)
	SLOC@LDA	−0.03	0.09	0.14	−1.48	5.76	−0.76 (BiF$_3$)
	mBJLDA@LDA	−0.07	0.10	0.24	−1.55	4.32	−3.42 (Ne)
	PBE@PBE	0.01	0.03	0.04	1.17	2.74	−0.25 (LaF$_3$)
	RPBE@PBE	0.00	0.02	0.04	0.16	2.33	−0.32 (SnTe)
	EV93@PBE	0.00	0.03	0.04	−0.18	2.24	−0.28 (SnTe)
	HLE16@PBE	−0.03	0.11	0.17	−1.75	6.12	−1.17 (NaCl)
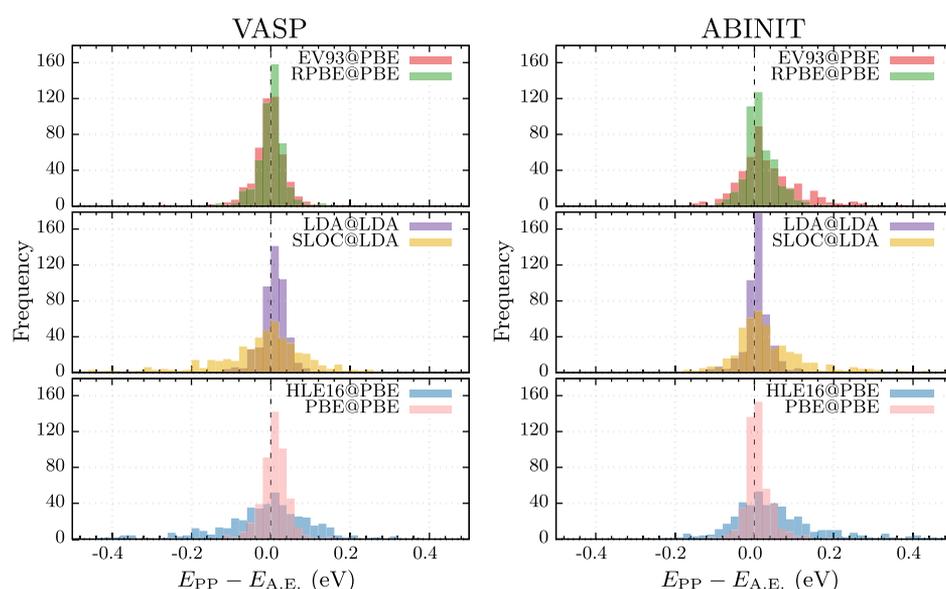
Figure 1. Histograms of errors (with respect to the all-electron results) for band gaps computed with VASP (left) and ABINIT (right). Boxes have a width of 0.02 eV.

accuracy). Although this set covers most of the periodic table, some elements such as thorium are absent and had, unfortunately, to be left out of the calculations. Because ABINIT does not currently support PPs with nonlinear core corrections for meta-GGAs, mBJLDA calculations with this code were not performed. For SLOC and HLE16, we generated a set of PPs using the ONCVPSP package[76] (version 3.3.1). As a starting point, we used the input files from the stringent set of the Pseudo Dojo distribution, changing them to include the desired functionals. Whenever we failed to generate a PP using the "stringent" input (*e.g.*, Br, Te, I, Rn, and La), we resorted to use the "standard" input. In practice, this leads to include less electrons in the valence. Further small changes to the local part of the PP were performed in order to avoid spurious effects (in particular, ghost states[77−79]) that were detected by the postprocessing tools of ONCVPSP. We note that although care was taken in this process, we did not perform further tests (Δ-test, GBVR test, *etc.*[18−20]) or optimizations. Therefore, although these PPs yield generally consistent results for band gaps, care should be taken for a more general use. The PPs are

given in the Supporting Information, and the whole set can also be downloaded from ref 80.

Note that the three codes, as well as ONCVPSP, are linked to the library of xc functionals LIBXC,[29,30] which allows us to access several hundreds of functionals, including the ones considered here.

All calculations were performed neglecting spin−orbit coupling. This term is expected to contribute on average about 0.1 eV to the band gap. This amount is considerably smaller than the typical average error of the xc functionals. Anyway, as all calculations were performed consistently without this term, its exclusion does not affect our comparison between the codes, which is the main purpose of the present work.

Statistics. For the analysis of the results, we compare band gaps calculated with norm-conserving PPs and PAW methods to all-electron values. Our analysis is restricted to the materials that were not determined by WIEN2k to have a theoretical band gap smaller than 0.01 eV, despite being measured to be semi-conductors. From the original 473 entries, WIEN2k predicts between 13 and 40 of such materials, depending on the functional.

Whenever presenting the results, we use the notation <functionals xc>@<pseudo xc>, and if the code used is ambiguous, we precede this string with its name. For example, ABINIT/PBE@LDA would make a reference to the set of values computed with ABINIT, using the PBE functionals with LDA PPs.

The statistical analysis is based on the determination of the mean absolute error, $MAE = \sum_{i=1}^{n}|y_i - y_{i,exp}|/n$; the mean error, $ME = \sum_{i=1}^{n}(y_i - y_{i,exp})/n$; the standard deviation of the errors, $\sigma = \sum_{i=1}^{n}(y_i - y_{i,exp} - ME)^2/n$; the median error (MnE); the interquartile range; the median of the absolute deviations from the median (MADM); the mean absolute percentage error; the mean percentage error; and the maximum absolute error in the calculation of band gaps with respect to experimental values. The complete set of results is presented in Tables SI−SVII of the Supporting Information, while Table 1 shows a summary of the most important statistical quantities.

After a preliminary analysis of the results, it became apparent that relative quantities (such as the MAPE) were being extremely affected by materials with very small band gaps. This is easy to understand as small errors lead to a rather large relative error for systems with band gaps smaller than 0.2 eV, skewing significantly the statistical averages. Therefore, we opted to consider, in Table 1, percentage quantities (MAPE and MPE) for the subset of systems with band gaps larger than 0.25 eV. Absolute quantities were still computed for the entire data set.

■ RESULTS

We start our analysis by looking at the results computed with the generally available LDA and PBE data sets. As visible in Table 1, band gap calculations performed with LDA and PBE xc functionals on top of the corresponding PPs are in excellent agreement with all-electron calculations. Not only are the MAE and ME for these calculations very small (in absolute value smaller than 0.03 eV) but also the dispersion of results is quite localized. This is visually represented in the error histograms of Figure 1 and also in the corresponding standard deviation σ (smaller than 0.06 eV). The maximum absolute error in these conditions is around 0.2−0.3 eV. However, one can see from the distribution of errors that absolute values larger than 0.1 eV are rare. These conclusions are valid for both PP and PAW calculations, although the MPE and MAPE of the latter are consistently larger. This may be explained by the fact that the Pseudo Dojo sets[75] are much more recent than the PAW sets available in VASP and that they were systematically optimized. In any case, these errors are certainly acceptable for the large majority of applications. This confirms the generally accepted idea that effective-core methods (either norm-conserving or PAW approach) are reliable for the calculations of band gaps.

Moving to the cross-functional calculations, we have to distinguish two different cases. Rather good results are still found for RPBE@PBE and EV93@PBE, which is probably due to the fact that the functional forms of RPBE and EV93 do not differ too much from PBE so that the PBE PPs are still accurate for RPBE and EV93. The increase in mean errors is the largest for EV93@PBE with ABINIT, 0.06 eV for the MAE, and 4.51% for the MAPE.

The situation is different for functionals that give accurate band gaps (HLE16, SLOC, and mBJLDA). Indeed, we can see a clear drop in accuracy, as seen by the increment in the various mean errors. For instance, the MAPE lies between 4.5 and 6.5% with both ABINIT and VASP, which is two or three times larger

than when LDA/PBE calculations are performed with a consistent PP. Note that these are still relatively small values, clearly smaller than the average errors with respect to experiment, which are of the order of 30%.[63] The loss in performance is more strikingly seen in terms of the dispersion of the errors (see Figure 1). In particular, the standard deviation σ reaches values in the range 0.14−0.24 eV, which represents a threefold increase. This increase in dispersion leads inevitably to an increase in the maximum error that can reach 1 eV or more, as shown in Tables 2 and 3. For example, ABINIT/SLOC@LDA

Table 2. List of the Ten Materials with the Highest Absolute Error (with Respect to the All-Electron Values)[a]

	ABINIT		
SLOC@LDA		HLE16@PBE	
material	error	material	error
$AlPO_4$	0.47 (7.75)	LaCuOTe	0.44 (0.65)
SiO_2	0.48 (7.70)	$ZnSnO_3$	0.44 (2.47)
LaCuOSe	0.51 (0.44)	GeO_2	0.45 (2.12)
Al_2O_3	0.52 (7.25)	ZnO	0.48 (2.82)
LaCuOS	0.55 (0.57)	LaCuOSe	0.52 (0.99)
$K_2La_2Ti_3O_{10}$	0.60 (1.17)	LaCuOS	0.56 (1.17)
La_2O_3	0.85 (1.89)	$NaLa_2TaO_6$	0.71 (2.63)
$NaLa_2TaO_6$	0.85 (1.73)	$CuLaO_2$	0.76 (2.38)
$CuLaO_2$	0.91 (1.75)	La_2O_3	0.77 (2.83)
LaF_3	1.33 (2.59)	LaF_3	1.10 (3.81)

[a]We consider here band gaps calculated with the ABINIT code using the SLOC and HLE16 functionals. The signed error is shown for each entry, and the all-electron band gap is indicated in parenthesis. All values are in eV.

and ABINIT/HLE16@PBE yield errors of 1.33 and 1.10 eV for LaF_3, respectively, corresponding to very large relative differences of ~50 and ~30%, respectively, with respect to WIEN2k values. VASP−PAW setups do not perform better. Maximum errors of −1.17 eV with VASP/HLE16@PBE (for NaCl) and −0.76 eV with VASP/SLOC@LDA (for BiF_3) are obtained. The situation is particularly worrying for mBJLDA@LDA, where we find a maximum deviation of −3.42 eV (for Ne) with respect to WIEN2k, while three other error values are above 1 eV. Curiously, ABINIT calculations tend to overestimate band gaps, while the reverse is true for VASP (see Tables 2 and 3 and Figure 1).

The solution to avoid such inaccuracies when using a new functional is rather clear and straightforward, namely, a PP has to be generated, optimized, and tested specifically for the new functional. This is what we have done for HLE16 and SLOC. The results are shown in Table 4, where we list the MAE, standard deviation σ, and MAPE for all functional combinations of LDA, PBE, HLE16, and SLOC. As expected, using an LDA potential in a PBE calculation or *vice versa* has relatively a small effect on the overall quality of the band gaps. However, using an inconsistent potential in a SLOC or HLE16 calculation has a much larger effect (by a factor of at least 3), confirming what was already discussed above. Because, grossly speaking, the difference between LDA and PBE results is smaller than the one between PBE/LDA and HLE16/SLOC, it is not entirely unexpected that an inconsistent PP for SLOC and HLE16 yields worse results. Performing consistent calculations brings back the PP error to the normal range (below 0.05 eV for the MAE and σ and at ~ 2% for the MAPE). Unfortunately, generating consistent PPs is far from obvious for more

Table 3. List of the Ten Materials with the Highest Absolute Error (with Respect to the All-Electron Values)[a]

		VASP			
SLOC@LDA		HLE16@PBE		mBJLDA@LDA	
material	error	material	error	material	error
$KTaO_3$	−0.43 (2.35)	ThO_2	−0.56 (3.83)	NaCl	−0.66 (8.38)
$LiTaO_3$	−0.44 (3.16)	$LiCoO_2$	−0.59 (1.18)	LiF	−0.68 (12.76)
$BaCl_2$	0.44 (5.86)	BiF_3	−0.60 (4.49)	KCl	−0.70 (8.48)
Ba_2InTaO_6	−0.45 (4.08)	La_2O_3	−0.63 (2.83)	SrF_2	−0.83 (11.04)
$NaTaO_3$	−0.45 (2.75)	$NaLa_2TaO_6$	−0.63 (2.63)	MgF_2	−0.84 (11.36)
HfO_2	−0.47 (4.31)	NaBr	−0.91 (6.45)	$AlPO_4$	−0.84 (9.10)
AgF	0.52 (3.07)	NaF	−0.93 (9.35)	NaF	−1.23 (11.48)
$Bi_2O_2CO_3$	−0.57 (0.97)	LaF_3	−1.01 (3.81)	Ar	−1.25 (13.79)
LaF_3	−0.67 (2.59)	NaI	−1.10 (5.69)	$LiIO_3$	−1.74 (4.91)
BiF_3	−0.76 (4.70)	NaCl	−1.17 (7.63)	Ne	−3.42 (22.27)

[a]We consider here band gaps calculated with the VASP code using the SLOC, HLE16, and mBJLDA functionals. The signed error is shown for each entry, and the all-electron band gap is indicated in parenthesis. All values are in eV.

Table 4. MAE (in eV), Standard Deviation σ (in eV), and MAPE (in %) with Respect to the All-Electron Results for the Band Gaps Obtained Using the ABINIT Code for all Cross-Functional PP Combinations

		functional			
		LDA	PBE	HLE16	SLOC
		MAE			
	LDA	0.02	0.05	0.12	0.08
	PBE	0.05	0.02	0.10	0.09
	HLE16	0.10	0.07	0.03	0.08
	SLOC	0.08	0.07	0.10	0.03
		σ			
	LDA	0.04	0.06	0.16	0.14
PP	PBE	0.06	0.03	0.14	0.16
	HLE16	0.14	0.11	0.04	0.12
	SLOC	0.13	0.13	0.13	0.05
		MAPE			
	LDA	2.47	4.88	7.79	5.43
	PBE	4.92	2.31	6.50	5.94
	HLE16	8.92	5.87	2.22	5.37
	SLOC	6.90	6.50	6.28	1.94

sophisticated methods such as hybrid functionals, many-body theories, or even the meta-GGA mBJLDA potential.

As the mBJLDA is currently the best performing semilocal functional for the prediction of band gaps,[63,71] a more detailed discussion is in order. The exchange component of mBJLDA (the correlation component consists of LDA) is essentially a rescaling of the Becke−Johnson[81] exchange potential *via* a density-dependent parameter c

$$v_x^{mBJ}(\mathbf{r}) = c v_x^{BR}(\mathbf{r}) + (3c - 2)\frac{1}{\pi}\sqrt{\frac{5}{6}}\sqrt{\frac{\tau(\mathbf{r})}{n(\mathbf{r})}} \quad (2)$$

where

$$c = \alpha + \beta\left[\frac{1}{V_{cell}}\int_{cell}\frac{|\nabla n(\mathbf{r}')|}{n(\mathbf{r}')}\,d\mathbf{r}'\right]^{1/2} \quad (3)$$

In eq 2, n is the electron density, τ is the kinetic energy density, and v_x^{BR} is the Becke−Roussel potential.[82] $\alpha = -0.012$ and $\beta = 1.023$ $Bohr^{1/2}$ are parameters which were fitted specifically for band gaps.[43] Originally, mBJLDA was implemented in an all-electron code, meaning that the quantities in eqs 2 and 3 are

defined with respect to the total density n and kinetic energy density τ of the system, comprising core and valence electrons. However, in the case of a PP code, such as ABINIT, one has to work with the pseudodensity n that differs significantly from the total density in the regions around the atoms (*i.e.*, it is much smoother). As such, it is doubtful that all-electron and PP calculations of eq 3 should give the same result. In fact, at the very least, the coefficients α and β should be reoptimized for pseudodensities (see, *e.g.*, ref 83 for such a procedure with ABINIT).

There is also some incongruousness within the VASP implementation of mBJLDA. Even if the PAW method allows us to recover the true density of the system theoretically, VASP performs an additive separation of c. This is certainly better than ignoring the contribution of the core density to c, but it is a numerical approximation. In practice, this leads to an underestimation of c (for most cases, see Figure S1) and therefore of the band gap (because the band gaps increase in a monotonous way with c). In order to illustrate the effect of an inaccurate value of c on the band gap more concretely, we show, in Table 5, the

Table 5. mBJLDA Band Gaps (in eV) Obtained with VASP and WIEN2k[a]

solid	VASP	VASP ($c = c_{WIEN2k}$)	WIEN2k
Ne	18.85	20.48	22.27
Ar	12.55	13.29	13.79
LiF	12.08	12.37	12.76
KCl	7.78	8.19	8.48
Al_2O_3	7.86	7.94	8.28

[a]The second set of VASP results were obtained with the parameter c in eq 2 fixed to the value obtained from the WIEN2k calculation.

mBJLDA band gap obtained with VASP and WIEN2k for some of the materials where the discrepancy between the two codes is the largest (from 1 to 4 eV). However, if the VASP calculations are performed by fixing the value of c to the one obtained from the WIEN2k calculation, then the band gap is clearly much closer to the WIEN2k value. For instance, for Ne, the VASP error gets reduced from about 3.5 to 1.8 eV. This shows that a large portion of the error with VASP is due to an inaccurate calculation of c.

The definition of the c parameter also creates some complications for the generation of an mBJLDA PP. As seen in eq 3, this parameter becomes ill-defined for (semi)finite

systems. This problem can however be bypassed. For example, Bartók and Yates[50] have recently proposed using a constant value for *c* during PP generation, obtaining good agreement with all-electron calculations. Another possible solution is the use of the localized version of the mBJLDA potential recently proposed in ref 51.

CONCLUSIONS

In summary, we performed a series of band gap calculations on a test set of 473 materials using all-electron, norm-conserving PP and PAW methods. Our goal was to estimate the error in the band gap when standard LDA/PBE PPs or PAW setups are used inconsistently to perform electronic structure calculations using other density functionals. From our results, we concluded the following.

1. As expected, consistent PP calculations are perfectly suited for the evaluation of band gaps. The errors with respect to the all-electron reference results (MAE ≈ 0.02 eV) are considerably smaller, by 1 or 2 orders of magnitude, than the errors (with respect to experiment) due to the approximation to the xc functional.

2. Using an inconsistent PP, that is, one that was generated and optimized for another xc functional, increases the mean absolute errors by a factor of 3 or more so that the MAE, for instance, can reach values around 0.1 eV. However, this is still smaller than the error due to other theoretical approximations, such as the choice of the xc functional; therefore, the PP approach is still justified for several applications, especially when one is interested in average quantities.

3. Nevertheless, the error in few specific (and unpredictable) cases can be quite large, with band gaps sometimes differing from the all-electron results by several eV. Therefore, when one requires precise numerical estimations of band gaps, the use of consistent PPs or all-electron calculations is strongly recommended.

Of course, these conclusions can be relevant not only for semilocal functionals; the use of inconsistent PPs with hybrid functionals, LDA + *U*, or many-body approaches such as GW should also be investigated more thoroughly.

The test set employed here did not contain magnetic materials. Effective-core methods are known to perform sometimes badly for these types of systems (*e.g.*, see ref 84). Preliminary calculations indicate that using the wrong PP in this situation can lead to errors as bad or worse than the ones observed here, but future tests are necessary to be able to properly quantify this effect.

As a final word, band gaps are only one of the many quantities of interest for the solid-state community. Large-scale studies of the effect of cross-functional calculations on other properties such as formation energies, geometries, absorption spectra, and so forth are important and should be encouraged. Only with access to such quantitative data, we can make informed decisions on the choice of methods for the calculation of electronic properties of materials.

ASSOCIATED CONTENT

ⓢ Supporting Information

The Supporting Information is available free of charge at https://pubs.acs.org/doi/10.1021/acs.jctc.0c00214.

Summary of the relevant statistical quantities for the different error distributions described in the main text and

comparison of *c* values from mBJLDA obtained using WIEN2k and VASP (PDF)

ABINIT PPs for HLE16 (ZIP)

Data set and calculated gaps (XLSX)

AUTHOR INFORMATION

Corresponding Authors

Miguel A. L. Marques − *Institut für Physik, Martin-Luther-Universität Halle-Wittenberg, D-06099 Halle, Germany;* ⓞ orcid.org/0000-0003-0170-8222; Email: miguel.marques@physik.uni-halle.de

Silvana Botti − *Institut für Festkörpertheorie und -optik, Friedrich-Schiller-Universität Jena and European Theoretical Spectroscopy Facility, 07743 Jena, Germany;* ⓞ orcid.org/0000-0002-4920-2370; Email: silvana.botti@uni-jena.de

Authors

Pedro Borlido − *Institut für Festkörpertheorie und -optik, Friedrich-Schiller-Universität Jena and European Theoretical Spectroscopy Facility, 07743 Jena, Germany;* ⓞ orcid.org/0000-0001-7675-3111

Jan Doumont − *Institute of Materials Chemistry, Vienna University of Technology, A-1060 Vienna, Austria*

Fabien Tran − *Institute of Materials Chemistry, Vienna University of Technology, A-1060 Vienna, Austria;* ⓞ orcid.org/0000-0003-4673-1987

Complete contact information is available at:
https://pubs.acs.org/10.1021/acs.jctc.0c00214

Notes

The authors declare no competing financial interest.

REFERENCES

(1) Hohenberg, P.; Kohn, W. Inhomogeneous Electron Gas. *Phys. Rev.* **1964**, *136*, B864−B871.

(2) Kohn, W.; Sham, L. J. Self-Consistent Equations Including Exchange and Correlation Effects. *Phys. Rev.* **1965**, *140*, A1133−A1138.

(3) Kümmel, S.; Kronik, L. Orbital-Dependent Density Functionals: Theory and Applications. *Rev. Mod. Phys.* **2008**, *80*, 3−60.

(4) Cohen, A. J.; Mori-Sánchez, P.; Yang, W. Challenges for Density Functional Theory. *Chem. Rev.* **2012**, *112*, 289−320.

(5) Burke, K. Perspective on density functional theory. *J. Chem. Phys.* **2012**, *136*, 150901.

(6) Becke, A. D. Perspective: Fifty years of density-functional theory in chemical physics. *J. Chem. Phys.* **2014**, *140*, 18A301.

(7) Yu, H. S.; Li, S. L.; Truhlar, D. G. Perspective: Kohn-Sham density functional theory descending a staircase. *J. Chem. Phys.* **2016**, *145*, 130901.

(8) Scuseria, G. E.; Staroverov, V. N. *Theory and Applications of Computational Chemistry*; Elsevier, 2005; pp 669−724.

(9) Pickett, W. E. Pseudopotential Methods in Condensed Matter Applications. *Comput. Phys. Commun.* **1989**, *9*, 115−197.

(10) Andrade, X.; et al. Real-Space Grids and the Octopus Code as Tools for the Development of New Simulation Approaches for Electronic Systems. *Phys. Chem. Chem. Phys.* **2015**, *17*, 31371−31396.

(11) Enkovaara, J.; et al. Electronic Structure Calculations with GPAW: A Real-Space Implementation of the Projector Augmented-Wave Method. *J. Phys.: Condens. Matter* **2010**, *22*, 253202.

(12) Blöchl, P. E. Projector Augmented-Wave Method. *Phys. Rev. B: Condens. Matter Mater. Phys.* **1994**, *50*, 17953−17979.

(13) Kresse, G.; Joubert, D. From Ultrasoft Pseudopotentials to the Projector Augmented-Wave Method. *Phys. Rev. B: Condens. Matter Mater. Phys.* **1999**, *59*, 1758−1775.

(14) Lippert, G.; Hutter, J. x. r.; Parrinello, M. The Gaussian and augmented-plane-wave density functional method for ab initio molecular dynamics simulations. *Theor. Chem. Acc.* **1999**, *103*, 124−140.

(15) Lippert, B. G.; Hutter, J.; Parrinello, M. A hybrid Gaussian and plane wave density functional scheme. *Mol. Phys.* **1997**, *92*, 477−488.

(16) Martin, R. M. *Electronic Structure: Basic Theory and Practical. Methods*; Cambridge University Press: Cambridge, 2004.

(17) Lejaeghere, K.; et al. Reproducibility in density functional theory calculations of solids. *Science* **2016**, *351*, aad3000.

(18) Garrity, K. F.; Bennett, J. W.; Rabe, K. M.; Vanderbilt, D. Pseudopotentials for High-Throughput DFT Calculations. *Comput. Mater. Sci.* **2014**, *81*, 446−452.

(19) Jollet, F.; Torrent, M.; Holzwarth, N. Generation of Projector Augmented-Wave Atomic Data: A 71 Element Validated Table in the XML Format. *Comput. Phys. Commun.* **2014**, *185*, 1246−1254.

(20) Lejaeghere, K.; Van Speybroeck, V.; Van Oost, G.; Cottenier, S. Error Estimates for Solid-State Density-Functional Theory Predictions: An Overview by Means of the Ground-State Elemental Crystals. *Crit. Rev. Solid State Mater. Sci.* **2014**, *39*, 1−24.

(21) Vosko, S. H.; Wilk, L.; Nusair, M. Accurate spin-dependent electron liquid correlation energies for local spin density calculations: a critical analysis. *Can. J. Phys.* **1980**, *58*, 1200−1211.

(22) Perdew, J. P.; Zunger, A. Self-Interaction Correction to Density-Functional Approximations for Many-Electron Systems. *Phys. Rev. B: Condens. Matter Mater. Phys.* **1981**, *23*, 5048−5079.

(23) Perdew, J. P.; Wang, Y. Accurate and Simple Analytic Representation of the Electron-Gas Correlation Energy. *Phys. Rev. B: Condens. Matter Mater. Phys.* **1992**, *45*, 13244−13249.

(24) Perdew, J. P.; Wang, Y. Erratum: Accurate and Simple Analytic Representation of the Electron-Gas Correlation Energy [Phys. Rev. B 45, 13244 (1992)]. *Phys. Rev. B* **2018**, *98*, 079904.

(25) Perdew, J. P.; Burke, K.; Ernzerhof, M. Generalized Gradient Approximation Made Simple. *Phys. Rev. Lett.* **1996**, *77*, 3865−3868.

(26) Hamann, D. R.; Schlüter, M.; Chiang, C. Norm-Conserving Pseudopotentials. *Phys. Rev. Lett.* **1979**, *43*, 1494−1497.

(27) Vanderbilt, D. Soft Self-Consistent Pseudopotentials in a Generalized Eigenvalue Formalism. *Phys. Rev. B: Condens. Matter Mater. Phys.* **1990**, *41*, 7892−7895.

(28) Perdew, J. P.; Ruzsinszky, A.; Csonka, G. I.; Vydrov, O. A.; Scuseria, G. E.; Constantin, L. A.; Zhou, X.; Burke, K. Restoring the Density-Gradient Expansion for Exchange in Solids and Surfaces. *Phys. Rev. Lett.* **2008**, *100*, 136406.

(29) Lehtola, S.; Steigemann, C.; Oliveira, M. J. T.; Marques, M. A. L. Recent Developments in Libxc — A Comprehensive Library of Functionals for Density Functional Theory. *SoftwareX* **2018**, *7*, 1−5.

(30) Marques, M. A. L.; Oliveira, M. J. T.; Burnus, T. Libxc: A Library of Exchange and Correlation Functionals for Density Functional Theory. *Comput. Phys. Commun.* **2012**, *183*, 2272−2281.

(31) Zunger, A.; Cohen, M. L. First-principles nonlocal-pseudopotential approach in the density-functional formalism: Development and application to atoms. *Phys. Rev. B: Condens. Matter Mater. Phys.* **1978**, *18*, 5449−5472.

(32) Bachelet, G. B.; Hamann, D. R.; Schlüter, M. Pseudopotentials that work: From H to Pu. *Phys. Rev. B: Condens. Matter Mater. Phys.* **1982**, *26*, 4199−4228.

(33) Topp, W. C.; Hopfield, J. J. Chemically Motivated Pseudopotential for Sodium. *Phys. Rev. B: Solid State* **1973**, *7*, 1295−1303.

(34) Starkloff, T.; Joannopoulos, J. D. Local pseudopotential theory for transition metals. *Phys. Rev. B: Solid State* **1977**, *16*, 5212−5215.

(35) Baybutt, P.; Bobrowicz, F. W.; Kahn, L. R.; Truhlar, D. G. Generalized valence-bond investigation of the reaction H+Br$_2$ → HBr +Br. *J. Chem. Phys.* **1978**, *68*, 4809−4822.

(36) Sun, J.; Ruzsinszky, A.; Perdew, J. P. Strongly Constrained and Appropriately Normed Semilocal Density Functional. *Phys. Rev. Lett.* **2015**, *115*, 036402.

(37) Adamo, C.; Barone, V. Toward Reliable Density Functional Methods without Adjustable Parameters: The PBE0 Model. *J. Chem. Phys.* **1999**, *110*, 6158−6170.

(38) Perdew, J. P.; Ernzerhof, M.; Burke, K. Rationale for Mixing Exact Exchange with Density Functional Approximations. *J. Chem. Phys.* **1996**, *105*, 9982−9985.

(39) Heyd, J.; Scuseria, G. E.; Ernzerhof, M. Hybrid Functionals Based on a Screened Coulomb Potential. *J. Chem. Phys.* **2003**, *118*, 8207−8215.

(40) Krukau, A. V.; Vydrov, O. A.; Izmaylov, A. F.; Scuseria, G. E. Influence of the Exchange Screening Parameter on the Performance of Screened Hybrid Functionals. *J. Chem. Phys.* **2006**, *125*, 224106.

(41) Hedin, L. New Method for Calculating the One-Particle Green's Function with Application to the Electron-Gas Problem. *Phys. Rev.* **1965**, *139*, A796−A823.

(42) Hybertsen, M. S.; Louie, S. G. Electron Correlation in Semiconductors and Insulators: Band Gaps and Quasiparticle Energies. *Phys. Rev. B: Condens. Matter Mater. Phys.* **1986**, *34*, 5390−5413.

(43) Tran, F.; Blaha, P. Accurate Band Gaps of Semiconductors and Insulators with a Semilocal Exchange-Correlation Potential. *Phys. Rev. Lett.* **2009**, *102*, 226401.

(44) Al-Saidi, W. A.; Walter, E. J.; Rappe, A. M. Optimized Norm-Conserving Hartree-Fock Pseudopotentials for Plane-Wave Calculations. *Phys. Rev. B: Condens. Matter Mater. Phys.* **2008**, *77*, 075112.

(45) Trail, J. R.; Needs, R. J. Norm-Conserving Hartree−Fock Pseudopotentials and Their Asymptotic Behavior. *J. Chem. Phys.* **2005**, *122*, 014112.

(46) Xu, X.; Holzwarth, N. A. W. Projector Augmented Wave Formulation of Hartree-Fock Calculations of Electronic Structure. *Phys. Rev. B: Condens. Matter Mater. Phys.* **2010**, *81*, 245105.

(47) Yang, J.; Tan, L. Z.; Rappe, A. M. Hybrid Functional Pseudopotentials. *Phys. Rev. B* **2018**, *97*, 085130.

(48) Tan, H.; Li, Y.; Zhang, S. B.; Duan, W. Effect of Hartree−Fock pseudopotentials on local density functional theory calculations. *Phys. Chem. Chem. Phys.* **2018**, *20*, 18844.

(49) Tan, H.; Liu, H.; Li, Y.; Duan, W.; Zhang, S. Understanding the origin of bandgap problem in transition and post-transition metal oxides. *J. Chem. Phys.* **2019**, *151*, 124703.

(50) Bartók, A. P.; Yates, J. R. Ultrasoft pseudopotentials with kinetic energy density support: Implementing the Tran-Blaha potential. *Phys. Rev. B* **2019**, *99*, 235103.

(51) Rauch, T.; Marques, M. A. L.; Botti, S. Local Modified Becke-Johnson Exchange-Correlation Potential for Interfaces, Surfaces, and Two-Dimensional Materials. *J. Chem. Theory Comput.* **2020**, *16*, 2654−2660.

(52) Anisimov, V. I.; Aryasetiawan, F.; Lichtenstein, A. I. First-principles calculations of the electronic structure and spectra of strongly correlated systems: the LDA+ U method. *J. Phys.: Condens. Matter* **1997**, *9*, 767.

(53) Anisimov, V. I.; Gunnarsson, O. Density-functional calculation of effective Coulomb interactions in metals. *Phys. Rev. B: Condens. Matter Mater. Phys.* **1991**, *43*, 7570.

(54) Yao, Y.; Kanai, Y. Plane-Wave Pseudopotential Implementation and Performance of SCAN Meta-GGA Exchange-Correlation Functional for Extended Systems. *J. Chem. Phys.* **2017**, *146*, 224105.

(55) Fuchs, M.; Bockstedte, M.; Pehlke, E.; Scheffler, M. Pseudopotential Study of Binding Properties of Solids within Generalized Gradient Approximations: The Role of Core-Valence Exchange Correlation. *Phys. Rev. B: Condens. Matter Mater. Phys.* **1998**, *57*, 2134−2145.

(56) Goedecker, S.; Saha, S. In *Handbook of Solid State Chemistry*; Dronskowski, R., Kikkawa, S., Stein, A., Eds.; Wiley-VCH Verlag GmbH & Co. KGaA: Weinheim, Germany, 2017; pp 29−58.

(57) Blaha, P.; Schwarz, K.; Madsen, G. K. H.; Kvasnicka, D.; Luitz, J.; Laskowski, R.; Tran, F.; Marks, L. D. *WIEN2k: An Augmented Plane Wave Plus Local Orbitals Program for Calculating Crystal Properties*; Vienna University of Technology: Austria, 2018.

(58) Blaha, P.; Schwarz, K.; Tran, F.; Laskowski, R.; Madsen, G. K. H.; Marks, L. D. WIEN2k: An APW+lo program for calculating the properties of solids. *J. Chem. Phys.* **2020**, *152*, 074101.

(59) Singh, D. J.; Nordström, L. *Planewaves, Pseudopotentials, and the LAPW Method*, 2nd ed.; Springer: New York, NY, 2006.

(60) Gonze, X.; et al. Recent Developments in the ABINIT Software Package. *Comput. Phys. Commun.* **2016**, *205*, 106−131.

(61) Gonze, X.; et al. The Abinitproject: Impact, environment and recent developments. *Comput. Phys. Commun.* **2020**, *248*, 107042.

(62) Kresse, G.; Furthmüller, J. Efficient Iterative Schemes for *Ab Initio* Total-Energy Calculations Using a Plane-Wave Basis Set. *Phys. Rev. B: Condens. Matter Mater. Phys.* **1996**, *54*, 11169−11186.

(63) Borlido, P.; Aull, T.; Huran, A. W.; Tran, F.; Marques, M. A. L.; Botti, S. Large-Scale Benchmark of Exchange−Correlation Functionals for the Determination of Electronic Band Gaps of Solids. *J. Chem. Theory Comput.* **2019**, *15*, 5069−5079.

(64) Finzel, K.; Baranov, A. I. A Simple Model for the Slater Exchange Potential and Its Performance for Solids. *Int. J. Quantum Chem.* **2017**, *117*, 40−47.

(65) Hammer, B.; Hansen, L. B.; Nørskov, J. K. Improved Adsorption Energetics within Density-Functional Theory Using Revised Perdew-Burke-Ernzerhof Functionals. *Phys. Rev. B: Condens. Matter Mater. Phys.* **1999**, *59*, 7413−7421.

(66) Engel, E.; Vosko, S. H. Exact Exchange-Only Potentials and the Virial Relation as Microscopic Criteria for Generalized Gradient Approximations. *Phys. Rev. B: Condens. Matter Mater. Phys.* **1993**, *47*, 13164−13174.

(67) Perdew, J. P.; Chevary, J. A.; Vosko, S. H.; Jackson, K. A.; Pederson, M. R.; Singh, D. J.; Fiolhais, C. Atoms, Molecules, Solids, and Surfaces: Applications of the Generalized Gradient Approximation for Exchange and Correlation. *Phys. Rev. B: Condens. Matter Mater. Phys.* **1992**, *46*, 6671−6687.

(68) Verma, P.; Truhlar, D. G. HLE16: A Local Kohn−Sham Gradient Approximation with Good Performance for Semiconductor Band Gaps and Molecular Excitation Energies. *J. Phys. Chem. Lett.* **2017**, *8*, 380−387.

(69) Slater, J. C. Simplification of the Hartree-Fock Method. *Phys. Rev.* **1951**, *81*, 385−390.

(70) Boese, A. D.; Handy, N. C. A New Parametrization of Exchange-Correlation Generalized Gradient Approximation Functionals. *J. Chem. Phys.* **2001**, *114*, 5497−5503.

(71) Tran, F.; Blaha, P. Importance of the Kinetic Energy Density for Band Gap Calculations in Solids with Density Functional Theory. *J. Phys. Chem. A* **2017**, *121*, 3318−3325.

(72) Verma, P.; Truhlar, D. G. HLE17: An Improved Local Exchange-Correlation Functional for Computing Semiconductor Band Gaps and Molecular Excitation Energies. *J. Phys. Chem. C* **2017**, *121*, 7144.

(73) Aschebrock, T.; Kümmel, S. Ultranonlocality and accurate band gaps from a meta-generalized gradient approximation. *Phys. Rev. Res.* **2019**, *1*, 033082.

(74) Jain, A.; Ong, S. P.; Hautier, G.; Chen, W.; Richards, W. D.; Dacek, S.; Cholia, S.; Gunter, D.; Skinner, D.; Ceder, G.; Persson, K. A. Commentary: The Materials Project: A materials genome approach to accelerating materials innovation. *APL Mater.* **2013**, *1*, 011002.

(75) van Setten, M. J.; Giantomassi, M.; Bousquet, E.; Verstraete, M. J.; Hamann, D. R.; Gonze, X.; Rignanese, G.-M. The PseudoDojo: Training and Grading a 85 Element Optimized Norm-Conserving Pseudopotential Table. *Comput. Phys. Commun.* **2018**, *226*, 39−54.

(76) Hamann, D. R. Optimized Norm-Conserving Vanderbilt Pseudopotentials. *Phys. Rev. B: Condens. Matter Mater. Phys.* **2013**, *88*, 085117.

(77) Gonze, X.; Käckell, P.; Scheffler, M. Ghost states for separable, norm-conserving, ab-initio pseudopotentials. *Phys. Rev. B: Condens. Matter Mater. Phys.* **1990**, *41*, 12264−12267.

(78) Gonze, X.; Stumpf, R.; Scheffler, M. Analysis of separable potentials. *Phys. Rev. B: Condens. Matter Mater. Phys.* **1991**, *44*, 8503−8513.

(79) Prandini, G.; Marrazzo, A.; Castelli, I. E.; Mounet, N.; Marzari, N. Precision and efficiency in solid-state pseudopotential calculations. *npj Comput. Mater.* **2018**, *4*, 72.

(80) https://tddft.org/bmg/data.php, 2020.

(81) Becke, A. D.; Johnson, E. R. A Simple Effective Potential for Exchange. *J. Chem. Phys.* **2006**, *124*, 221101.

(82) Becke, A. D.; Roussel, M. R. Exchange Holes in Inhomogeneous Systems: A Coordinate-Space Model. *Phys. Rev. A: At., Mol., Opt. Phys.* **1989**, *39*, 3761−3767.

(83) Traoré, B.; Bouder, G.; Lafargue-Dit-Hauret, W.; Rocquefelte, X.; Katan, C.; Tran, F.; Kepenekian, M. Efficient and accurate calculation of band gaps of halide perovskites with the Tran-Blaha modified Becke-Johnson potential. *Phys. Rev. B* **2019**, *99*, 035139.

(84) Kresse, G.; Blaha, P.; Da Silva, J. L. F.; Ganduglia-Pirovano, M. V. Comment on "Taming multiple valency with density functionals: A case study of defective ceria". *Phys. Rev. B: Condens. Matter Mater. Phys.* **2005**, *72*, 237101.